DEVELOPMENT OF THE VORTEX METHOD FOR CENTRIFUGAL IMPELLER APPLICATIONS

Luiz Antonio Alcântara Pereira, luizantp@unifei.eu.br
Institute of Mechanical Engineering, Federal University of Itajuba, Itajuba, Minas Gerais, Brazil, CP 50

Miguel Hiroo Hirata, hirata@superonda.com.br
State University of Rio de Janeiro, FAT-UERJ, Resende, Rio de Janeiro, Brazil

Abstract. *In the present study, the two-dimensional features of the viscous flow through a centrifugal impeller are investigated numerically by using vortex method. Lifting of the restriction to introduce the periodicity of the blade-to-blade flow here permits the natural development of circumferential flow variations from blade-to-blade. The near wake analysis is carried out in order to understand the dynamics of the vortex formation process in the wake.*

Keywords*: discrete vortex method, vorticity shedding, near wake, radial-flow impeller*

1. INTRODUCTION

Many of numerical works have used vortex method to study moving boundaries at high Reynolds number. A typical example of this kind is the flow within a turbomachinery. For a radial-flow impeller configuration the moving boundaries are the blades of impeller which rotate with respect to the stator and/or to the spiral casing. Understanding of the vortex-shedding flow behind blades of impeller is of great fundamental and practical importance to design of turbomachines. The impeller-viscous wake interaction originates from the impingement and the convection of the wakes shed from the preceding blades in the relative motion. A large number of detailed experimental investigations and theoretical or numerical studies are reported in the literature to unsteady flow investigation in turbomachines. However, most of these efforts concern the unsteadiness in axial turbomachines.

In order to solve the turbomachines problem numerically, we can use either Eulerian or Lagrangian methods. In the past three decades, the vortex methods have been developed and applied for analysis of complex vortical flows, because they are standing on simple algorithm based on physics of flows and their numerical stability is usually quite well, and it should be noted that grid generation in the flow field is not necessary (Kamemoto, 2004). A cloud of free vortices is used in order to simulate the vorticity, which is generated on the body surface and develops into the boundary layer and the viscous wake. Each individual free vortex of the cloud is followed during the numerical simulation in a typical Lagrangian scheme. Important features of the vortex methods (Chorin, 1973; Leonard, 1980; Sarpkaya, 1989; Sethian, 1991; Lewis, 1999; Alcântara Pereira *et al.*, 2002; Kamemoto, 2004; Stock, 2007; hirata *et al.*, 2008) are:

(i) it is a numerical technique suitable for the solution of convection/diffusion type equations like the Navier-Stokes ones;

(ii) it is a suitable technique for direct simulation and large-eddy simulation;

(iii) it is a mesh free technique; the vorticity field is represented by a cloud of discrete free vortices that move with the fluid velocity.

Vortex cloud simulation offers a number of advantages over the more traditional Eulerian schemes for the analysis of the external flow that develops in a large domain; the main reasons are:

(i) as a fully mesh-less scheme, no grid is necessary;

(ii) the computational efforts are directed only to the regions with non-zero vorticity and not to all the domain points as is done in the Eulerian formulations;

(iii) the far away downstream boundary condition is taken care automatically which is relevant for the simulation of the flow around a bluff body (or an oscillating body) that has a wide viscous wake.

The first application of the vortex method to turbomachinery blade rows, including the prediction of rotating stall in compressors and vibrations induced by blade row wake interaction, was published by Lewis and Porthouse (1983) and Porthouse (1983) followed by some fairly comprehensive studies by Sparlat (1984).

Lewis (1989) presented a basic scheme for vortex cloud modeling of cascades assuming that the boundary layers and wakes developed by the blades of an infinite cascade are identical. As the coupling coefficients are periodic in the y direction, surface elements and discrete vortex shedding need only be considered for the reference airfoil. The surface of the reference airfoil was represented by straight-line elements, with a point vortex located at the pivotal point. The vorticity diffusion that occurs in the wake was simulated using random walk method. The pressure on the airfoil surface was calculated according inviscid flow analysis. Although predicted surface pressure agrees well with experiment for the turbine cascade, losses are over-predicted. Due to "numerical stall", Lewis (1989) approach proved inadequate to deal with the compressor cascade.

In the paper presented by Alcântara Pereira *et al.* (2004), the surface of the reference airfoil was represented by straight-line panels, with a constant density vortex distribution on them. A new approach to the pressure calculation was presented to that one used by Lewis (1989). This approach represents an enhancement to the previous ones not only due to the more accurate computed values, but also because it allows one to compute the pressure distribution on the body surface as well as in the whole fluid domain; this feature can be of fundamental importance in many engineering problems. In order to take into consideration the effects of the phenomena that take place in the micro scales a new methodology was presented. With this methodology one can consider the effects of turbulence in the flow that develops in and around complex geometry structures. The vortex method, a particle or Lagrangian method was used in combination with a sub grid scale modeling for turbulence that employs a second-order velocity structure function of the filtered field, see Alcântara Pereira *et al.* (2002).

In the all above studies, the assumption was made that each blade flow was identical, a not unreasonable assumption for unstalled turbine or fan blade rows. For off-design angles of attack leading to stall it is know that there can significant blade-to-blade variations. Lewis (2004) extended the analysis to deal with such situations.

On the other hand, Zhu *et al.* (1998) presented a new procedure to simulate the vorticity transport near a centrifugal impeller boundary using vortex method. In their paper, a number of nascent vortices were introduced according to diffusion and convection vorticity near the boundary. The two-dimensional unsteady features of the whole flow field were solved without introducing the periodicity of a blade-to-blade flow. The results showed how the separation of boundary layer develops into a strong vortex structure and how the vortex is periodically shed and moves and produces an oscillatory flow in a blade-to-blade passage.

In a recent paper, Putini *et al.* (2008) introduced geometrical simplifications to prediction of the two-dimensional unsteady flow established in a radial flow centrifugal pump; more specifically, the blades were represented by NACA 0012 base profile. In this paper, the vortex method developed by Hirata *et al.* (2008) is extended to simulate the vorticity transport near blade boundaries of shape of one-circular-arc camber without introducing the periodicity of a blade-to-blade flow.

2. FORMULATION OF THE PHYSICAL PROBLEM

2.1. Definitions

Consider the fluid flow around a two-dimensional radial-flow pump impeller as shown in Fig. 1. The volumetric flow rate per unit breadth of the impeller is established considering a point source located at (x, y) = (0, 0). Figure 1 shows that the (x, o, y) is the inertial frame of reference and the (ξ, o, η) is the coordinate system fixed to the impeller; this coordinate system rotate clockwise, being $\varphi_t = \lambda t$ and λ the angular velocity of the impeller.

The boundary S of the fluid domain is $S = S_b \cup S_\infty$; being S_∞ the far away boundary, which can be viewed as $r = \sqrt{x^2 + y^2} \to \infty$, and S_b the blades surface.

In the impeller fixed coordinate system, the surface S_b is defined by

$$\begin{Bmatrix} \xi \\ \eta \end{Bmatrix} = \begin{Bmatrix} \cos(\varphi_t) & \sin(\varphi_t) \\ -\sin(\varphi_t) & \cos(\varphi_t) \end{Bmatrix} \begin{Bmatrix} x \\ y \end{Bmatrix}. \tag{1}$$

2.2. Governing Equations

For an incompressible fluid flow the continuity is written as

$$\nabla \cdot \mathbf{u} = 0 \tag{2}$$

where $\mathbf{u} \equiv (u, v)$ is the velocity vector.

If, in addition, the fluid is Newtonian with constant properties the momentum equation is represented by the Navier-Stokes equation as

$$\frac{\partial \mathbf{u}}{\partial t} + \mathbf{u} \cdot \nabla \mathbf{u} = -\nabla p + \frac{1}{Re} \nabla^2 \mathbf{u} . \tag{3}$$

Here, p is the pressure field and Re stands for the Reynolds number defined as $Re = \frac{D_2 V_0}{\upsilon}$, where υ is the kinematic viscosity of fluid , V_0 is defined as radial velocity at the entrance of the impeller for the design point and D_2 is defined as outer diameter of the impeller.

On the impeller surface the adherence condition has to be satisfied. This condition is better specified in terms of the normal and tangential components as

$(\mathbf{u}\cdot\mathbf{n}) = (\mathbf{v}\cdot\mathbf{n})$ on S_b, the impenetrability condition (4)

$(\mathbf{u}\cdot\boldsymbol{\tau}) = (\mathbf{v}\cdot\boldsymbol{\tau})$ on S_b, the no-slip condition (5)

where **n** and **τ** are unit normal and tangential vectors and **v** is the blade surface velocity vector.

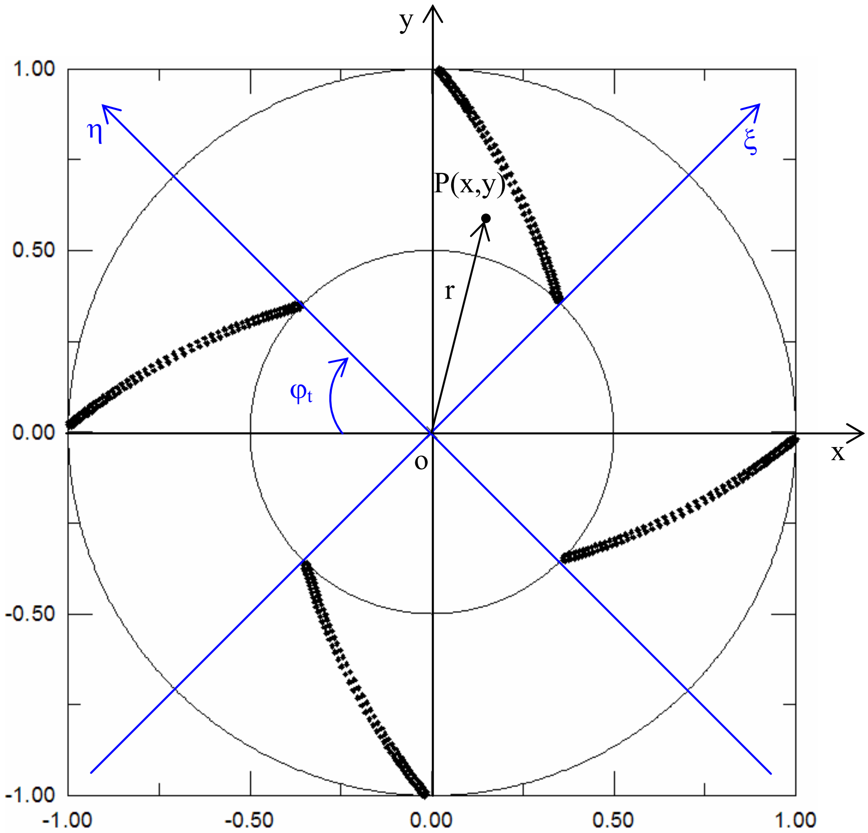

Figure 1 – Definitions of the physical domain

Far from the impeller (for $r \to \infty$, in Fig. 1) one assumes that the perturbation due to the rotation impeller fades away, that is

$$|\mathbf{u}| \to 0 \ . \tag{6}$$

One should mention that the above boundary value problem was made non-dimensional using V_0 and D_2 as characteristic quantities. Normalized non-dimensional time t is defined as $t = \dfrac{TV_0}{D_2}$, where T is the time elapsed after revolution of the impeller starting at a constant speed.

3. THE VORTEX METHOD

3.1. Viscous Splitting Algorithm (Chorin, 1973)

Taking the curl of the Navier-Stokes equation and with some algebraic manipulations one gets the vorticity equation which presents no pressure term. In two-dimensions this equation reads

$$\frac{\partial \omega}{\partial t} + \mathbf{u}\cdot\nabla\omega = \frac{1}{Re}\nabla^2\omega \tag{7}$$

where $\omega(\mathbf{x}, t) = \nabla\times\mathbf{u}(\mathbf{x}, t)$ represents the only non-zero component of the vorticity field (observe that the pressure is absent from the formulation).

The left hand side of the above equation carries all the information needed for the convection of vorticity while the right hand side governs the diffusion. Following Chorin (1973) we use the viscous splitting algorithm, which, for the same time step of the numerical simulation, says that

Convection of vorticity is governed by

$$\frac{\partial\omega}{\partial t} + \mathbf{u}\cdot\nabla\omega = 0\,, \tag{8}$$

Diffusion of vorticity is governed by

$$\frac{\partial\omega}{\partial t} = \frac{1}{Re}\nabla^2\omega\,. \tag{9}$$

3.2. Convection and diffusion of vorticity

The vortex method proceeds by discretizing spatially the vorticity field using a cloud of elemental vortices, which are characterized by a distribution of vorticity, ς_{σ_i} (commonly called the cutoff function), the circulation strength Γ_i and the core size σ_i. Thus, the discretized vorticity is expressed by

$$\omega(\mathbf{x},t) \approx \omega^h(\mathbf{x},t) = \sum_{i=1}^{Z}\Gamma_i(t)\varsigma_{\sigma_i}(\mathbf{x}-\mathbf{x}_i(t)). \tag{10}$$

where Z is the number of point vortices of the cloud used to simulate the vorticity field.

In this paper, as the diffusion effects are simulated using the random displacement method (Lewis, 1999), we assume that the core sizes are uniform ($\sigma_i = \sigma$), and use the Gaussian distribution as the cut-off function; this choice of the cut-off function leads to the Lamb Vortices (Leonard, 1980); thus

$$\varsigma_\sigma(\mathbf{x}) = \frac{1}{\pi\sigma^2}\exp\left(-\frac{|\mathbf{x}|^2}{\sigma^2}\right). \tag{11}$$

The numerical analysis is conducted over a series of small discrete time steps Δt for each of which a discrete vortex element $\Gamma_{(i)}$ is shed from each impeller surface element. The intensity $\Gamma_{(i)}$ of these newly generated vortices is determined using the no-slip condition, see Eq. (5).

For the convection of the discrete vortices of the cloud, Eq. (8) is written in its Lagrangian form as

$$\frac{dx^{(i)}}{dt} = u^{(i)}(x,y,t)\,, \tag{12}$$

$$\frac{dy^{(i)}}{dt} = v^{(i)}(x,y,t) \tag{13}$$

being (i) = 1, Z.

A second order solution to this equation is given by the Adams-Bashforth formula (Ferziger, 1981)

$$x^{(i)}(t+\Delta t) = x^{(i)}(t) + \left[1.5u^{(i)}(t) - 0.5u^{(i)}(t-\Delta t)\right]\Delta t\,, \tag{14}$$

$$y^{(i)}(t+\Delta t) = y^{(i)}(t) + \left[1.5v^{(i)}(t) - 0.5v^{(i)}(t-\Delta t)\right]\Delta t\,. \tag{15}$$

The diffusion of vorticity is taken care of using the random walk method. The random displacement $Z_d \equiv (x_d, y_d)$, with a zero mean and a $(2\Delta t/Re)$ variance, for vortex (i) is defined as

$$x_d^{(i)} = [\cos(2\pi Q)]\sqrt{\frac{4\Delta t}{Re}\ln\left(\frac{1}{P}\right)}, \tag{16}$$

$$y_d^{(i)} = [\sin(2\pi Q)]\sqrt{\frac{4\Delta t}{Re}\ln\left(\frac{1}{P}\right)} \tag{17}$$

where P and Q are random numbers in the range 0.0 to 1.0. Therefore the final displacement is written as

$$x^{(i)}(t+\Delta t) = x^{(i)}(t) + \left[1.5u^{(i)}(t) - 0.5u^{(i)}(t-\Delta t)\right]\Delta t + x_d^{(i)}, \tag{18}$$

$$y^{(i)}(t+\Delta t) = y^{(i)}(t) + \left[1.5v^{(i)}(t) - 0.5v^{(i)}(t-\Delta t)\right]\Delta t + y_d^{(i)}. \tag{19}$$

3.3. Numerical Implementation

The $u^{(i)}$ and $v^{(i)}$ components of the velocity induced at the location of the vortex (i) can be written as

$$u^{(i)} = ur^{(i)} + ub^{(i)} + uv^{(i)}, \tag{20}$$

$$v^{(i)} = vr^{(i)} + vb^{(i)} + vv^{(i)} \tag{21}$$

where, $\mathbf{ur}^{(i)} \equiv [ur^{(i)}, vr^{(i)}]$ is the velocity vector of the radial direction,

$\mathbf{ub}^{(i)} \equiv [ub^{(i)}, vb^{(i)}]$ is the velocity vector induced by the impeller at the location of vortex (i),

$\mathbf{uv}^{(i)} \equiv [uv^{(i)}, vv^{(i)}]$ is the velocity vector induced at the vortex (i) due to the vortex cloud.

The $ur^{(i)}$ and $vr^{(i)}$ calculations present no problems. The impeller contributes with $\mathbf{ub}(\mathbf{x}, t)$, which can be obtained, for example, using the Boundary Element Method (Katz and Plotkin, 1991). The two components can be written as

$$ub^{(i)} = \sum_{k=1}^{NP} \psi_k uc_k^{(i)}, \tag{22}$$

$$vb^{(i)} = \sum_{k=1}^{NP} \psi_k vc_k^{(i)} \tag{23}$$

where NP is the total number of flat source panels representing impeller. It is assumed that the source strength per length is constant such that ψ_k = const and $uc_k^{(i)}$ and $vc_k^{(i)}$ are the components of the velocity induced at vortex (i) by a unit strength flat source panel located at k.

As the each blade surface is simulated by NB straight line panels (Panels Method) it is convenient to calculate the impeller induced velocity in the moving coordinate system. For that one has to observe the following

- The fluid velocity on the each blade surface is written as

$$\mathbf{u}(\xi, \eta; t) = (ur + u_\lambda)\mathbf{i} + (vr - v_\lambda)\mathbf{j}. \tag{24}$$

As a consequence of impeller rotation components of the right hand side of the fluid velocity (in the above expression) one gets an additional singularities distribution on the each blade surface. Of course, the induced velocity due to this additional singularities distribution fades away from the each blade.

- The velocity induced by the impeller, according to the Panels Method calculations, is indicated by [ub(ξ,η), vb(ξ,η)]; this is the velocity induced at the vortex (i), located at the point [ξ(t), η(t)]; thus

$$ub^{(i)}(x, y; t) = ub(\xi, \eta; t) - u_\lambda, \tag{25}$$

$$vb^{(i)}(x, y; t) = vb(\xi, \eta; t) + v_\lambda \tag{26}$$

where the following relations remains

$$\begin{Bmatrix} x \\ y \end{Bmatrix}^{(i)} = \begin{Bmatrix} \cos(\varphi_t) & -\sin(\varphi_t) \\ \sin(\varphi_t) & \cos(\varphi_t) \end{Bmatrix} \begin{Bmatrix} \xi \\ \eta \end{Bmatrix}^{(i)} . \tag{27}$$

Finally, the velocity **uv** is obtained from the vorticity field by means of the Biot-Savart law

$$\mathbf{uv}(\mathbf{x},t) = \int (\nabla \times \mathbf{G})(\mathbf{x}-\mathbf{x'})\omega(\mathbf{x'},t)d\mathbf{x'} = \int \mathbf{K}(\mathbf{x}-\mathbf{x'})\omega(\mathbf{x'},t)d\mathbf{x'} = (\mathbf{K}*\omega)(\mathbf{x},t) \tag{28}$$

where $\mathbf{K} = \nabla\times\mathbf{G}$ is the Biot-Savart kernel, **G** is the Green's function for the Poisson equation, and $*$ represents the convolution operation.

4. RESULTS AND DISCUSSION

The numerical simulations were restricted to the interference effects between four blades whose shape consists of one-circular-arc camber and constant thickness as three percent of the radius of the camber-arc. In the Fig. 2, the inlet diameter is given as $D_1 = 0.5D_2$, the inlet blade angel is β_1=30° and the outlet angle is β_2=50°. Each blade was modeled by one hundred (NB=100) straight-line source panels with constant density. The time increment was Δt=0.05 and the nascent vortices were placed into the cloud through a displacement $\varepsilon=\sigma_0=0.0001D_1$ normal to the panels, see Ricci (2002). For infinite Reynolds number viscous effects would have a little influence. For the impeller Reynolds number of 1.0×10^5 selected here on the other hand, viscous diffusion will differ considerably due to radial velocity diffusion.

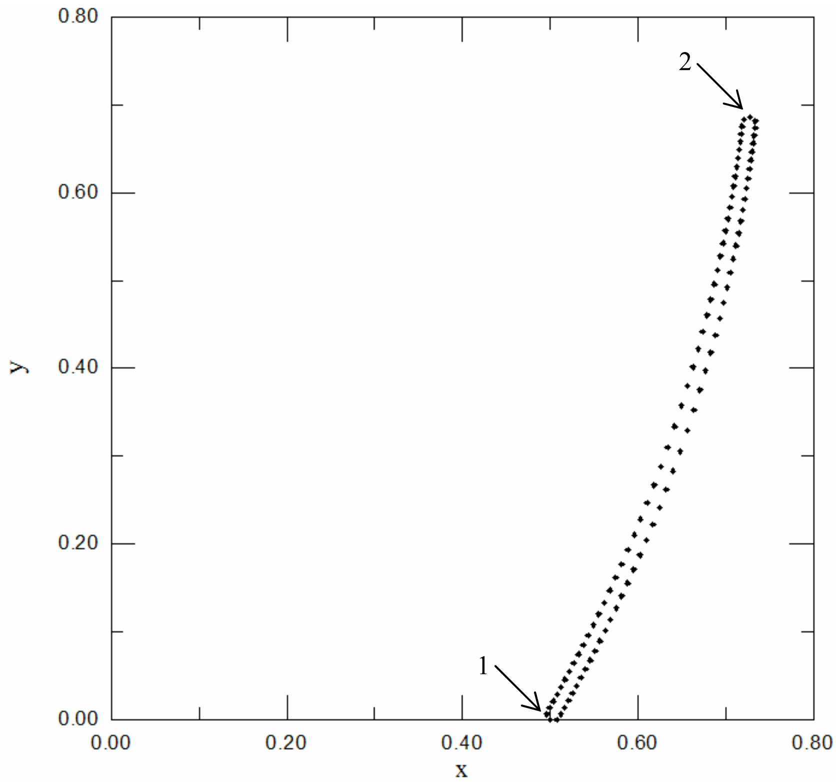

Figure 2 – Format for blade boundary configuration using NB=100 straight-line panels

Figure 3 shows the development of the vortex structures in a centrifugal impeller with four blades. The angular velocity of the impeller and the volumetric flow rate per unit breadth of the impeller were λ=0.05 and Q=2.0, respectively. In this example the impeller was rotated clock-wise with zero pre-whirl but with sufficient angular velocity.

As can be seen from the predicted flow pattern after 100 time steps, see Fig. 3(c), there is clear the evidence of cluster of free vortices formed due to the flow separation from an impeller surface with some circumferential variation from blade to blade. After a period of time as motion proceeds, we observe in the Fig. 3(d) the development of vortex structures which propagate in the radial direction. The reason for this behavior can be deduced from the vortex dynamics simulation demonstrating the power of this CFD technique for prediction and diagnosis.

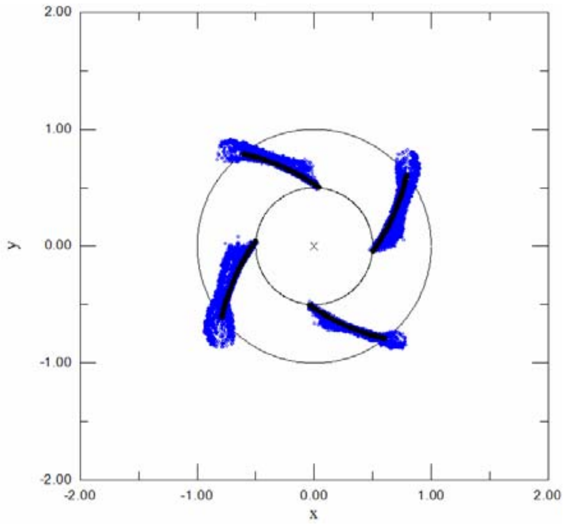

(a) t=2.0

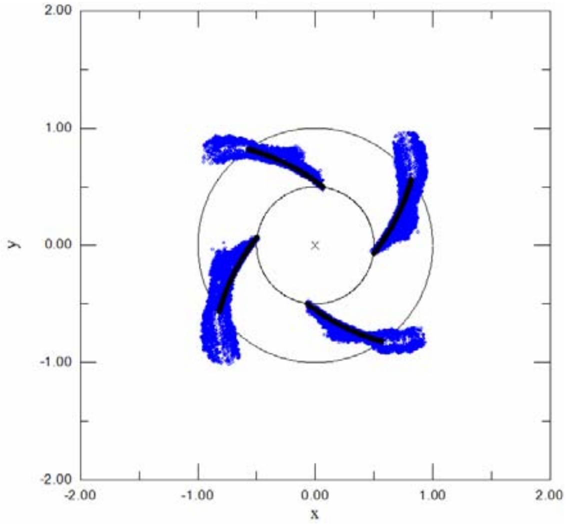

(b) t=3.0

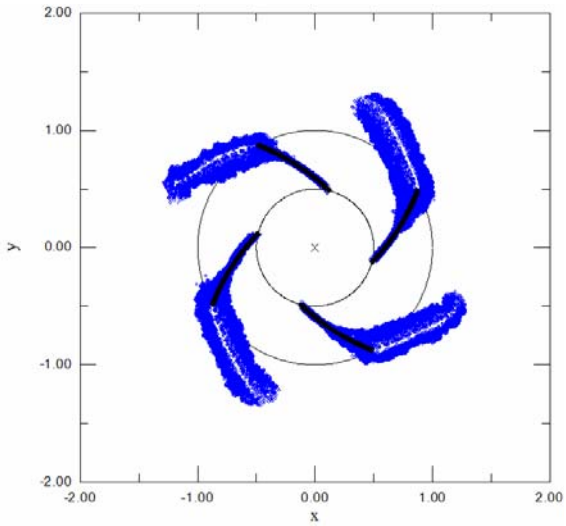

(c) t=5.0

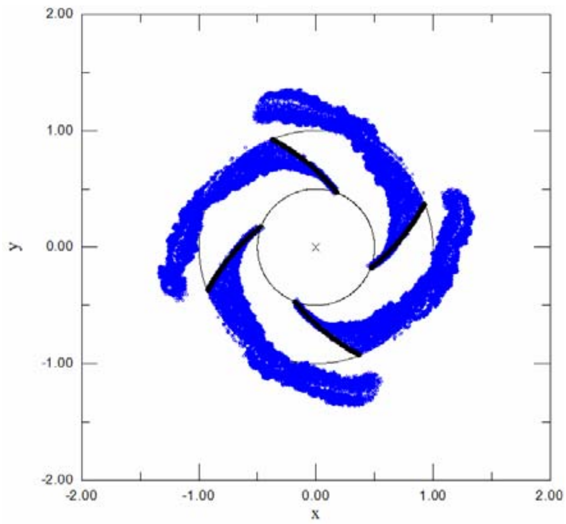

(d) t=7.5

Figure 3 – Vortex cloud analysis of a centrifugal impeller at Re=1.0×10^5

In the case of a centrifugal fan it can expect that these stall cells would cause serious fluctuating interference with the stator and be a serious source of unwanted vibrations. Numerical techniques to predict unsteady flow characteristics of an impeller have been desired since before, for design and improvement of operation performance. The vortex code has been developed here shows potentialities to predict flow separation in a blade-to-blade passage.

Figure 4 presents the predicted flow pattern at t=9.5. It is clarified that there are differences among the flows around individual profile, whereas the whole flow field is calculated without introducing the approximation of the periodicity of the blade-to-blade flow. Choice of the group of blades is then a matter of computational limitations including available memory, time of execution and numerical accuracy available for vortex code.

Because the distributed vorticity of the mainstream flow has been replaced in the numerical model by a cloud of discrete vortices, the CPU time for vortex-vortex interaction turns expensive. No attempts to simulate the flow for NB greater than 100 were made since the operation count of our algorithm is proportional to the square of Z. As NB increases Z also tends to increase, and the computational efforts becomes expensive. This is a major source of difficulties, and it can only be handled through the utilization of faster schemes for the induced velocity calculations, such as the multipole technique (Greengard and Rokhlin, 1987) and/or parallel computers to run long simulations (Takeda *et al.*, 1999).

In order to solve the pressure Poison equation, a simple method based on the boundary element method will be carried out (Uhlman, 1992; Kamemoto, 1993; Shintani and Akamatsu, 1994).

Finally, the results are promising and encourage performing additional tests in order to explore the phenomena in more details. Future work will investigate the influence of shape of one-circular-arc camber and the thickness of the blades.

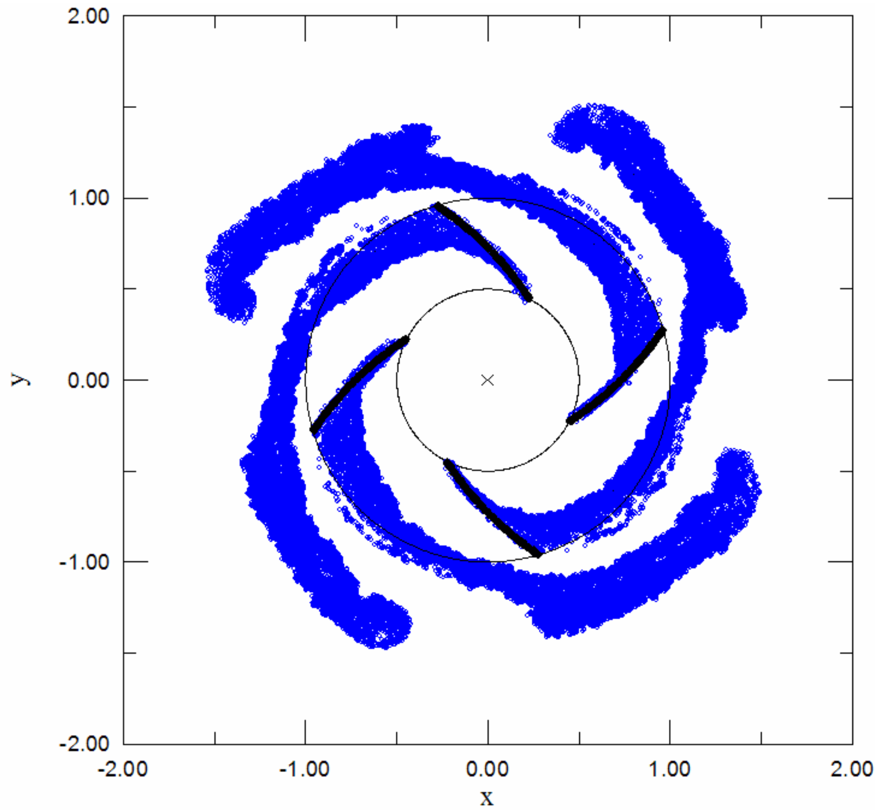

Figure 4 – Vortex flow pattern at t=9.5.

5. CONCLUSIONS AND SUMMARY

The main conclusions that can be drawn are:

(i) The model used in the numerical simulations (although with a simple geometrical form) can be applied to analysis of unsteady characteristics and occurrence of unsymmetrical flow through a centrifugal impeller. In this paper, two-dimensional unsteady features of the flow were computed without introducing the periodicity of a blade-to-blade flow. Using this representation, a grid-free (Lagrangian) numerical method was derived based on the coupling of the boundary element and vortex particle methods. The main objective of the work was to implement the algorithm and to get some insight into the potentialities of the model developed; this was accomplished since the results show that the behavior of the rotating stall cells propagation in a centrifugal impeller is the expected one. It is clearly demonstrated in Figure 4 that the flow becomes non-axis-symmetrical and some of blade-to-blade passages seem to be blocked with separation bubbles.

(ii) The experience gained with the present work allows one to analyze complex situations where relative motions between impeller-blades and guide vanes and/or volute casing are present. These extend the applicability of the numerical code.

(iii) The use of a fast summation scheme to compute the velocities of the vortex elements, such as the multiple expansions, allows an increase in the number of vortices and a reduction of the time step, which increases the resolution of the simulation, in addition to a reduction of the CPU time, which allows a longer simulation time to be carried out.

(iv) The use of global as well local quantities combined to the near field flow pattern observations will be used to understand the complex mechanisms that lead the origin and the time evolution of the aerodynamic loads.

6. ACKNOWLEDGEMENTS

This research was supported by the CNPq (Brazilian Research Agency) Proc. 470420/2008-1, FAPERJ (Research Foundation of the State of Rio de Janeiro) Proc. E-26/112/013/2008 and FAPEMIG (Research Foundation of the State of Minas Gerais) Proc. TEC APQ-01074-08.

7. REFERENCES

Alcântara Pereira, L.A., Hirata, M.H. and Manzanares Filho, N., 2004, "Wake and Aerodynamics Loads in Multiple Bodies - Application to Turbomachinery Blade Rows", J. Wind Eng. Ind. Aerodyn., 92, pp. 477-491.

Alcântara Pereira, L.A., Ricci, J.E.R., Hirata, M.H. and Silveira-Neto, A., 2002, "Simulation of Vortex-Shedding Flow about a Circular Cylinder with Turbulence Modeling", Intern'l Society of CFD, Vol. 11, No. 3, October, pp. 315-322.

Chorin, A.J., 1973, "Numerical Study of Slightly Viscous Flow", Journal of Fluid Mechanics, Vol. 57, pp. 785-796.

Ferziger, J.H., 1981, "Numerical Methods for Engineering Application", John Wiley & Sons, Inc.

Greengard, L. and Rokhlin, V., 1987, "A Fast Algorithm for Particle Simulations", Journal of Computational Physics, Vol. 73, pp. 325-348.

Hirata, M. H., Alcântara Pereira, L. A., Recicar, J. N., Moura, W. H., 2008, "High Reynolds Number Oscillations of a Circular Cylinder", J. of the Braz. Soc. Of Mech. Sci. & Eng., Vol. XXX, No. 4, pp. 300-308.

Kamemoto, K., 2004, "On Contribution of Advanced Vortex Element Methods Toward Virtual Reality of Unsteady Vortical Flows in the New Generation of CFD", Proceedings of the 10th Brazilian Congress of Thermal Sciences and Engineering-ENCIT 2004, Rio de Janeiro, Brazil, Nov. 29 - Dec. 03, Invited Lecture-CIT04-IL04.

Kamemoto, K., 1993, "Procedure to Estimate Unstead Pressure Distribution for Vortex Method" (In Japanese), Trans. Jpn. Soc. Mech. Eng., Vol. 59, No. 568 B, pp. 3708-3713.

Katz, J. and Plotkin, A., 1991, "Low Speed Aerodynamics: From Wing Theory to Panel Methods". McGraw Hill, Inc.

Leonard, A., 1980, "Vortex Methods for Flow Simulation", J. Comput. Phys., Vol. 37, pp. 289-335.

Lewis, R.I., 2004, "Study of Blade to Blade Flows and Circumferential Stall Propagation in Radial Diffusers and Radial Fans by Vortex Cloud Analysis", Journal of Computational and Applied Mechanics, Vol. 5, no.2 , pp. 323-335.

Lewis, R.I., 1999, "Vortex Element Methods, the Most Natural Approach to Flow Simulation - A Review of Methodology with Applications", Proceedings of 1st Int. Conference on Vortex Methods, Kobe, Nov. 4-5, pp. 1-15.

Lewis, R.I., 1989, "Application of the Vortex Cloud Method to Cascades". Int. J. Turbo & Jet Engine, vol. 6, pp. 231-245.

Lewis, R.I. and Porthouse, D.T.C., 1983, "Numerical Simulation of Stalling Flows by an Integral Equation Method". AGARD Meeting. Viscous Effects in Turbomachines, AGARD-CPP-351, Copenhagen.

Porthouse, D.T.C., 1983, Numerical Simulation of Aerofoil and Bluff Body Flows by Vortex Dynamics. University of Newcastle upon Tyne, England, UK, Ph. D. Thesis.

Putini, E.P.G., Alcântara Pereira, L.A. and Hirata, M.H., 2008, "Application of the Vortex Method to Centrifugal Pump Impeller", 12th Brazilian Congress of Thermal Engineering and Sciences, November, 10-14, Belo Horizonte, MG, Brazil.

Ricci, J.E.R., 2002, "Numerical Simulation of the Flow around a Body in the Vicinity of a Plane Using Vortex Method", Ph.D. Thesis, Mechanical Engineering Institute, UNIFEI, Itajubá, MG, Brazil (in Portuguese).

Sarpkaya, T., 1989, "Computational Methods with Vortices - The 1988 Freeman Scholar Lecture", Journal of Fluids Engineering, Vol. 111, pp. 5-52.

Sethian, J.I., 1991, "A Brief Overview of Vortex Method, Vortex Methods and Vortex Motion", SIAM. Philadelphia, pp. 1-32.

Shintani, M. and Akamatsu, T, 1994, "Investigation of Two Dimensional Discrete Vortex Method with Viscous Diffusion Model", Computational Fluid Dynamics Journal, Vol. 3, No. 2, pp. 237-254.

Sparlat, P.R., 1984, "Two Recent Extensions of the Vortex Method". A.I.A.A., 22nd Aerospace Sciences Meeting, Reno, Nevada, A.I.A.A. Paper 84-034.3.

Stock, M.J., 2007, "Summary of Vortex Methods Literature (A lifting document rife with opinion)", April, 18: © 2002-2007 Mark J. Stock.

Takeda, K., Tutty, O.R. and Nicole, D.A., 1999, "Parallel Discrete Vortex Method on Commodity Supercomputers; an Investigation into Bluff Body Far Wake Behaviour", ESAIM: Proceedings, Third International Workshop on Vortex Flows and Related Numerical Methods, Vol. 7, pp. 418-428.

Uhlman, J.S., 1992, "An Integral Equation Formulation of the Equation of an Incompressible Fluid", Naval Undersea Warfare Center, T.R. 10-086.

Zhu, B.S, Kamemoto, K. and Matsumoto, H., 1998, "Direct Simulation of Unsteady Flow through a Centrifugal Pump Impeller Using a Fast Vortex Method". Computational Fluid Dynamics Journal, Vol. 7, No. 1, April, pp. 15-26.

8. RESPONSIBILITY NOTICE

The author(s) is (are) the only responsible for the printed material included in this paper.